

## Supporting Information

# Hierarchical hybrid monolith: MoS<sub>4</sub><sup>2-</sup>-intercalated NiFe layered double hydroxide nanosheet arrays assembled on carbon foam for highly efficient heavy metal removal

Yongchuang Wang,<sup>a,b</sup> Yue Gu,<sup>a,b</sup> Donghua Xie,<sup>a,b</sup> Wenxiu Qin,<sup>a</sup> Haimin Zhang,<sup>a</sup> Guozhong Wang,<sup>a</sup> Yunxia Zhang<sup>a,\*</sup> and Huijun Zhao<sup>a,c</sup>

<sup>a</sup> Key Laboratory of Materials Physics, Centre for Environmental and Energy Nanomaterials, Anhui Key Laboratory of Nanomaterials and Nanotechnology, CAS Centre for Excellence in Nanoscience, Institute of Solid State Physics, Chinese Academy of Sciences, Hefei 230031, China.

<sup>b</sup> University of Science and Technology of China, Hefei 230026, P. R. China

<sup>c</sup> Centre for Clean Environment and Energy, Gold Coast Campus, Griffith University, Queensland 4222, Australia.

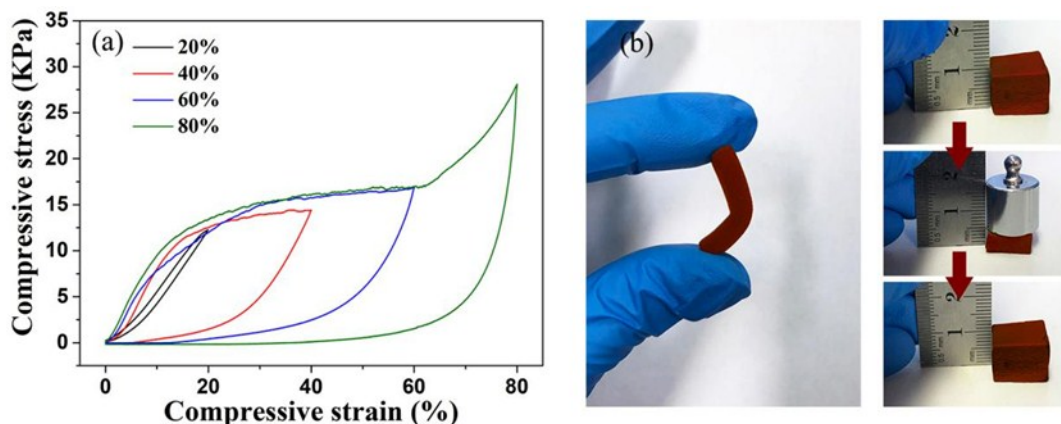


**Fig. S1** (a) Compressive stress-strain curves of the 3D NiFe-MoS<sub>4</sub><sup>2-</sup>-LDH/CF hybrid monolith at strain values of 20, 40, 60, 80%; (b) Digital photograph of the obtained 3D NiFe-MoS<sub>4</sub><sup>2-</sup>-LDH/CF hybrid monolith after the bending and compressive treatments.

\* Correspondence Author. Email: [yxzhang@issp.ac.cn](mailto:yxzhang@issp.ac.cn)  
Fax: +86-551-65591434; Tel: +86-551-65592145

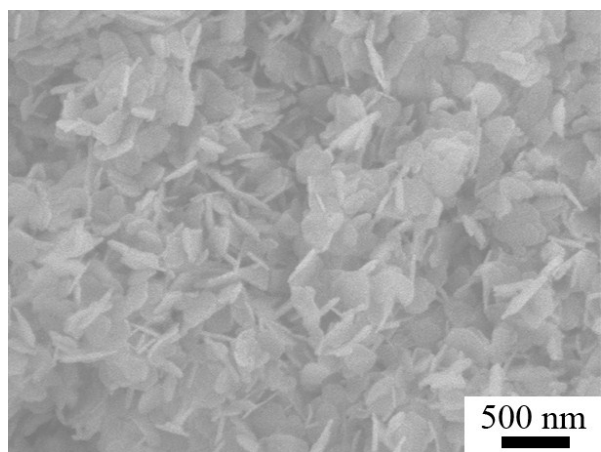


**Fig. S2** FESEM image of NiFe-MoS<sub>4</sub><sup>2-</sup>-LDH in the absence of CF.

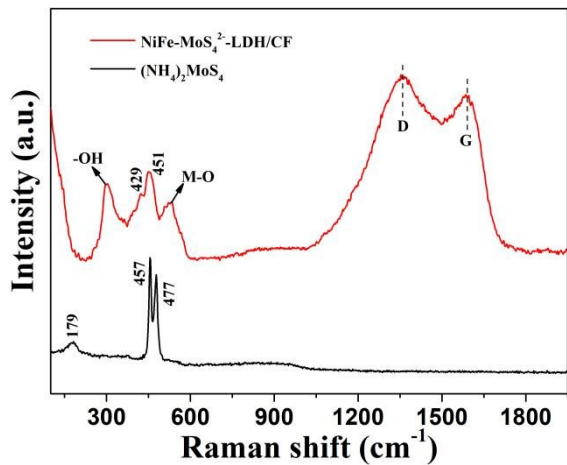


**Fig. S3** Raman spectra of the obtained NiFe-MoS<sub>4</sub><sup>2-</sup>-LDH/CF and pure (NH<sub>4</sub>)<sub>2</sub>MoS<sub>4</sub>.

**Table S1** Langmuir and Freundlich isotherm parameters for Cu<sup>2+</sup>, Pb<sup>2+</sup> and Hg<sup>2+</sup> on NiFe-MoS<sub>4</sub><sup>2-</sup>-LDH/CF.

ions	Langmuir model		Freundlich model			
	Q <sub>max</sub> (mg/g)	K <sub>L</sub> (L/mg)	R <sup>2</sup>	K <sub>F</sub> (mg/g)	1/n	R <sup>2</sup>
Hg <sup>2+</sup>	462.08	0.0849	0.9994	139.27	0.3059	0.9389
Pb <sup>2+</sup>	298.73	0.0561	0.9953	60.83	0.2872	0.9074
Cu <sup>2+</sup>	127.56	0.0383	0.9911	26.88	0.2241	0.9354

**Table S2** Comparison of sorption kinetic parameters of various adsorbents.

Target ions	Adsorbents	Initial concentration (ppm)	Adsorbent dosage (g/L)	Removal efficiency (%)	Time of sorption equilibrium (min)	References
$\text{Hg}^{2+}$	LHMS-1	0.0637	0.5	96.9	30	1
	KMS-1	0.116	1	99.8	40	2
	KMS-2	885.8	~	99.9	180	3
	$\text{MoS}_4$ -LDH	27.1	1.17	99.8	60	4
	Fe-MoS <sub>4</sub>	200	1	99	120	5
	mercaptosuccinic acid-LDH	100	~	99	60	6
	Active carbon	20	~	91.85	105	7
	NiFe-MoS <sub>4</sub> <sup>2-</sup> -LDH/CF	10	0.5	99.9	20	This work
$\text{Pb}^{2+}$	$\text{Mg}_2\text{Al}$ -LS-LDH	50	0.5	72.8	120	8
	Fe-MoS <sub>4</sub>	200	1	99	120	5
	$\text{MoS}_4$ -LDH	19.2	1.17	99.7	30	4
	Modified alkaline lignin	1-30	1	95	100	9
	KMS-1	0.061	1	99.8	120	2
	TCAS-LDHs	50	0.5	93.9	120	10
	NiFe-MoS <sub>4</sub> <sup>2-</sup> -LDH/CF	10	0.5	99.9	20	This work
$\text{Cu}^{2+}$	$\text{Mg}_2\text{Al}$ -LS-LDH	50	0.5	47	120	8
	nano-alumina	80	4	61.25	30	11
	Fe-MoS <sub>4</sub>	200	1	54	120	5
	$\text{MoS}_4$ -LDH	20.3	1.17	99.9	120	4
	MGL	80	3.5	7.86	240	12
	MNP-NH <sub>2</sub>	2-10	0.1	27-75	5	13
	TCAS-LDHs	50	0.5	60.3	120	10
	NiFe-MoS <sub>4</sub> <sup>2-</sup> -LDH/CF	10	0.5	99	30	This work

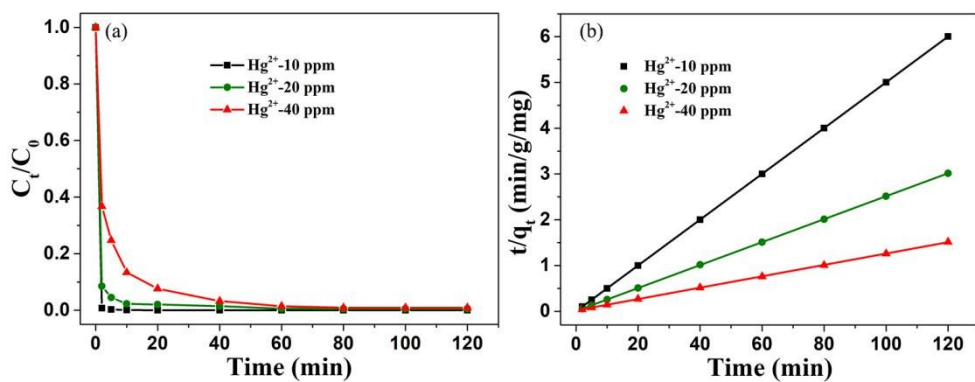


**Fig. S4** (a) Adsorption kinetics of  $\text{Hg}^{2+}$  with different initial concentration; (b) the corresponding fitting curves via pseudo-second-order kinetics model. Experimental condition: 0.5 g/L of sorbent dosage, pH value 6.0, and temperature 298 K.

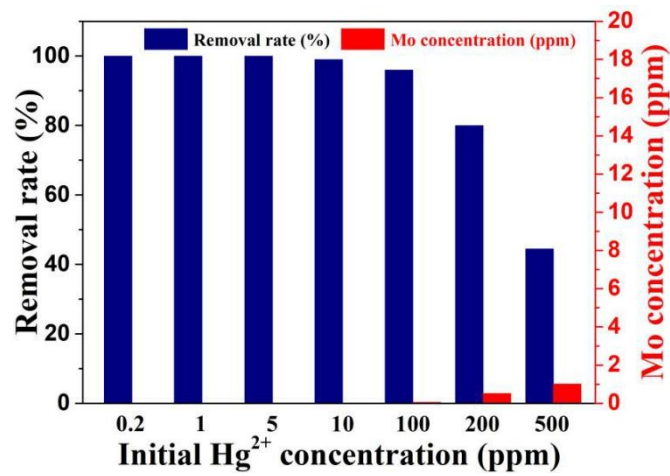


**Fig. S5** The removal rate of  $\text{Hg}^{2+}$  with various initial concentrations on NiFe-MoS<sub>4</sub><sup>2-</sup>-LDH/CF and Mo concentration in the filtrations after adsorption.

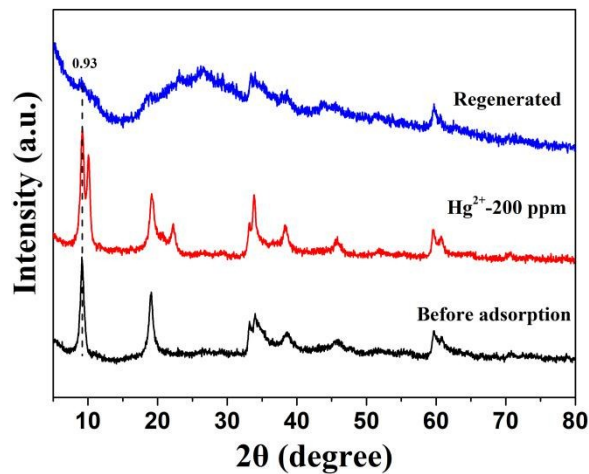
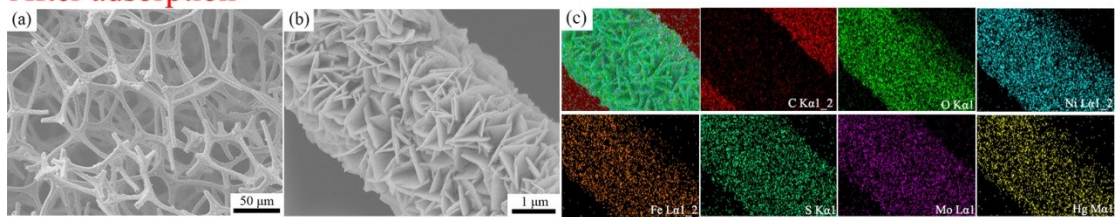


**Fig. S6** XRD patterns of NiFe-MoS<sub>4</sub><sup>2-</sup>-LDH/CF before and after  $\text{Hg}^{2+}$  adsorption as well as the regenerated sample after 5 cycles.

### After adsorption



### After regeneration

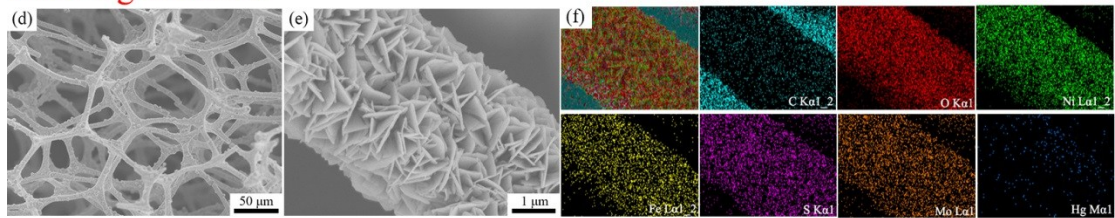


**Fig. S7** SEM images and corresponding EDS element mappings of NiFe-MoS<sub>4</sub><sup>2-</sup>-LDH/CF during adsorption-regeneration cycles.

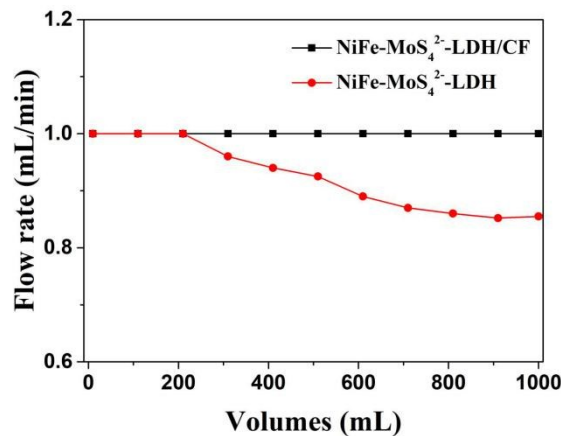


**Fig. S8** The real-time flow rate in the fixed bed adsorption experiment.

**Table S3** Parameters of the Thomas model in the column studies.

Factors	Q (mL min <sup>-1</sup> )	Initial concentration	K <sub>TH</sub> (mL min <sup>-1</sup> mg <sup>-1</sup> )	R <sup>2</sup>	q <sub>0</sub> (mg g <sup>-1</sup> )
<b>Flow rate</b>	1	5 ppm	0.0030	0.9994	45.95
	2	5 ppm	0.0058	0.9988	44.01
	4	5 ppm	0.0141	0.9983	36.57
<b>Initial concentration</b>	1	0.2 ppm	0.0137	0.9993	8.664
	1	1 ppm	0.0035	0.9921	31.72
	1	5 ppm	0.0030	0.9994	45.95

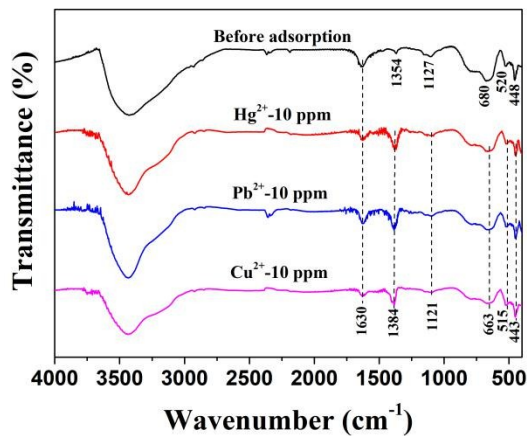


**Fig. S9** FT-IR spectrum of NiFe-MoS<sub>4</sub><sup>2-</sup>-LDH/CF after the uptake of various heavy metal ions.

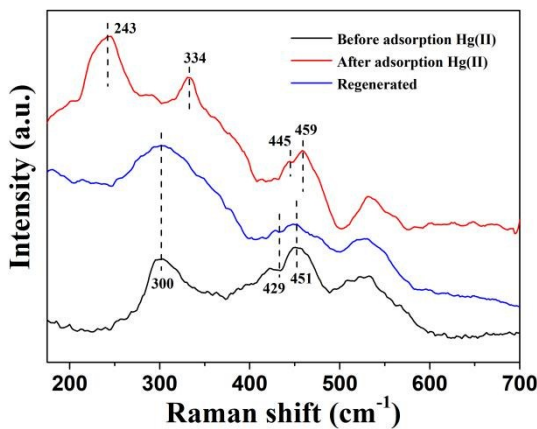


**Fig. S10** Raman spectra of NiFe-MoS<sub>4</sub><sup>2-</sup>-LDH/CF before and after Hg<sup>2+</sup> adsorption as well as the regenerated sample.

**Table S4** The atomic percentages of Ni, Fe, Mo, S and Hg on NiFe-MoS<sub>4</sub><sup>2-</sup>-LDH/CF solid treated by different concentration of Hg<sup>2+</sup> solution.

	Ni (at%)	Fe (at%)	Mo (at%)	S (at%)	Hg (at%)
<b>Before adsorption</b>	15.92	5.38	2.16	8.71	~
<b>1 ppm Hg</b>	15.89	5.37	2.15	8.69	0.04
<b>10 ppm Hg</b>	15.76	5.32	2.11	8.62	0.14
<b>100 ppm Hg</b>	15.66	5.28	2.06	8.37	0.66
<b>500 ppm Hg</b>	15.42	5.27	1.67	7.13	1.82

## Notes and references

- 1 M. J. Manos, V. G. Petkov and M. G. Kanatzidis, *Adv. Funct. Mater.*, 2009, **19**, 1087–1092.
- 2 M. J. Manos and M. G. Kanatzidis, *Chem. Eur. j.*, 2009, **15**, 4779–4784.
- 3 Z. H. Fard, C. D. Malliakas, J. L. Mertz and M. G. Kanatzidis, *Chem. Mater.*, 2015, **27**, 1925–1928.
- 4 L. Ma, Q. Wang, S. M. Islam, Y. Liu, S. Ma and M. G. Kanatzidis, *J. Am. Chem. Soc.*, 2016, **138**, 2858–2866.
- 5 A. Jawad, Z. Liao, Z. Zhou, A. Khan, T. Wang, J. Ifthikar, A. Shahzad, Z. Chen and Z. Chen, *ACS Appl. Mater. Interfaces*, 2017, **9**, 28451–28463.
- 6 H. Nakayama, S. Hirami, M. Tsuhako, *J. Colloid. Interf. Sci.*, 2007, **315**, 177–183.
- 7 K. Kadirvelu, M. Kavipriya, C. Karthika, N. Vennilamani and S. Pattabhi, *Carbon*, 2004, **42**, 745–752.
- 8 G. Huang, D. Wang, S. Ma, J. Chen, L. Jiang and P. Wang, *J. Colloid. Interf. Sci.*, 2015, **445**, 294–302.
- 9 Q. Wang, C. Zheng, Z. Shen, Q. Lu, C. He, T. C. Zhang and J. Liu, *Chem. Eng. J.*, 2019, **359**, 265–274.
- 10 G. Huang, L. Jiang, D. Wang, J. Chen, Z. Li and S. Ma, *J. Mol. Liq.*, 2016, **220**, 346–353.
- 11 R. Wang, W. Zhang, L. Zhang, T. Hua, G. Tang, X. Peng and M. Hao, *Environ. Sci. Pollut. R.*, 2019, **26**, 1595–1605.
- 12 Q. Q. Huang, Y. Chen, H. Q. Yu, L. G. Yan, J. H. Zhang, B. Wang, B. Du and L. T. Xing, *Chem. Eng. J.*, 2018, **341**, 1–9.
- 13 Y. M. Hao, M. Chen and Z. B. Hu, *J. Hazard. Mater.*, 2010, **184**, 392–399.